Published in final edited form as:

Nat Neurosci. 2009 August ; 12(8): 988–995. doi:10.1038/nn.2358.

A Discrete Alcohol Pocket Involved in GIRK Channel Activation

Prafulla Aryal[1,3], **Hay Dvir**[2], **Senyon Choe**[2], and **Paul A. Slesinger**[1,3]

[1]Peptide Biology Laboratory, The Salk Institute for Biological Studies, La Jolla, CA 92037

[2]Structural Biology Laboratory, The Salk Institute for Biological Studies, La Jolla, CA 92037

[3]Graduate Program in Biology, Division of Biology, University of California, San Diego, La Jolla, CA 92093.

Abstract

Ethanol modifies neural activity in the brain by modulating ion channels. Ethanol activates G protein-gated inwardly rectifying K^+ channels, but the molecular mechanism is not well understood. Here, we used a crystal structure of a mouse inward rectifier containing a bound alcohol and structure-based mutagenesis to probe a putative alcohol-binding pocket located in the cytoplasmic domains of GIRK channels. Substitutions with bulkier side-chains in the alcohol-binding pocket reduced or eliminated activation by alcohols. By contrast, alcohols inhibited constitutively open channels, such as IRK1 or GIRK2 that binds PIP_2 strongly. Mutations in the hydrophobic alcohol-binding pocket of these channels had no effect on alcohol-dependent inhibition, suggesting an alternate site is involved in inhibition. Comparison of high-resolution structures of inwardly rectifying K^+ channels suggests a model for activation of GIRK channels utilizing this hydrophobic alcohol-binding pocket. These results provide a tool for developing therapeutic compounds that could mitigate the effects of alcohol.

Keywords

ethanol; potassium channel; addiction; gating; hydrophobic-pocket; analgesia

Introduction

Many ligand-gated ion channels, such as those gated by gamma-aminobutyric acid (GABA), N-methyl-D-aspartate (NMDA), glycine, acetylcholine and serotonin, are responsive to ethanol (EtOH) and other alcohols1-4. Initially, alcohol was hypothesized to indirectly alter the function of channels by changing the fluidity of the lipid bilayer5. More recent studies, however, suggest alcohol acts directly through a physical-binding pocket located in the

Corresponding authors: Paul A. Slesinger (slesinger@salk.edu) and Senyon Choe (choe@salk.edu). Telephone: 858−453−4100 (x1560 or x1652).

Author Contributions

P.A.S. and P.A. designed the experiments and analyzed the data. P.A. conducted the molecular cloning, electrophysiology and imaging experiments. H.D. and P.A. collaborated on structural analysis and figure production. H.D. conducted modeling experiment. P.A., H.D., and P.A.S co-wrote and revised the manuscript. P.A.S and S.C. supervised the project.

channel protein3,6. In addition to ligand-gated channels, alcohols also modulate potassium channels7-9. For example, EtOH activates G protein-gated inwardly rectifying potassium (GIRK or Kir3) channels7,8. Behavioral studies have shown that mice lacking GIRK2 channels exhibit diminished EtOH-dependent analgesia10 and consume more EtOH than wild-type mice11, suggesting a functional role for GIRK channels in response to alcohols *in vivo*.

GIRK channels are also activated following stimulation of G protein-coupled receptors (GPCR) such as m2 muscarinic receptors (m2R). The mechanism of G protein activation has been extensively studied. Agonist binding to the GPCR leads to activation of the pertussis toxin sensitive G protein heterotrimer ($G\alpha\beta\gamma$), allowing the $G\beta\gamma$ subunits to associate directly with the channel and induce channel activation12,13. Mutagenesis and chimeric studies have identified several regions in the cytoplasmic domains of GIRK channels involved in $G\beta\gamma$ binding and activation14-19. Interestingly, pertussis-toxin treatment, which prevents GPCR-mediated G protein activation of GIRK channels, does not prevent alcohol activation8. These experiments suggest that alcohol activation occurs through a mechanism distinct from G protein activation.

Similar to GABA-gated ion channels, a physical pocket in the channel with a defined cutoff is postulated to mediate alcohol activation of GIRK channels. That is, alcohols with a carbon chain length up to four carbons (i.e. methanol, ethanol, 1-propanol (1-PrOH) and 1-butanol (1-BuOH)) activate GIRK1/2 heteromeric channels while longer alcohols inhibit the channels7,8. This cutoff effect suggests there are physical constraints, possibly linked to the length or hydrophobicity of the alcohol, that determine the sensitivity to alcohol modulation6,8. However, the molecular mechanism underlying alcohol activation of GIRK channels is not known. Mutagenesis studies of GIRK2 channels have implicated the distal C-terminal cytoplasmic domain in activation by alcohol7,20, but these studies did not reveal a physical alcohol-binding pocket in the channel.

Recently, we described a high resolution structure of the cytoplasmic domains of a G protein-insensitive inwardly rectifying potassium channel (IRK1 or Kir2.1) that contains bound alcohols21. The alcohol, 2-methyl-2,4-pentanediol (MPD), is bound to four similar solvent accessible hydrophobic pockets, each formed by two adjacent subunits of the tetramer. Intriguingly, this IRK1-bound pocket has features similar to the structure of an odorant alcohol binding protein, LUSH, which was crystallized with EtOH22. In both structures, the alcohol pocket is formed by hydrophobic amino acids and hydrogen bonding polar groups. Thus, the hydrophobic alcohol-bound pocket in IRK1 is a putative site for modulation by alcohols. Because the crystal structure of the cytoplasmic domain of GIRK1 or GIRK2 channels is very similar to that of IRK123-25, we hypothesize that GIRK channels also possess cytoplasmic hydrophobic alcohol-binding pockets that are involved in alcohol-dependent activation.

Results

Conservation of MPD bound pocket in IRK1 and GIRK2

Recently, we showed that a high resolution structure of the IRK1 cytoplasmic domains contains bound alcohols (which we refer to here as IRK1-MPD)21. The alcohol-binding pocket in the IRK1-MPD complex is formed by hydrophobic amino acid side-chains from three different domains, the N-terminal, the βD-βE ribbon and the βL-βM ribbon (Fig. 1a,b)24. There are seven amino acids that interact with MPD21. Of these, the hydrophobic side-chains of F47, L232, L245 and L330 and Y337 point toward the pocket. In addition to the hydrophobic environment of the pocket, hydrogen bonds may form between one of the hydroxyl groups of MPD and a hydrogen bonding triangle between backbone carbonyl of P244 and OH group of Y242 via a water and between the second hydroxyl group of MPD and the hydroxyl group of Y33721. We compared the high-resolution structure of IRK1 with that of GIRK225 and identified the putative alcohol-binding pocket in GIRK2. The hydrophobic pocket in GIRK2 has significant conservation with amino acids that line the pocket in IRK1 and appears large enough to accommodate MPD similar to IRK1 (Fig. 1c,d).

MPD activates GIRK2 channels similar to primary alcohols

To test whether the hydrophobic pocket in GIRK2 is the site for alcohol-mediated activation, we first investigated whether GIRK2 channels are sensitive to MPD modulation. Whereas primary alcohols up to the size of butanol (1-BuOH; four carbons) activate GIRK1/2 channels7,8, the effect of MPD with five backbone carbons was unknown. GIRK2 channels expressed in HEK-293T cells produced a small inwardly rectifying basal K^+ current that was inhibited by extracellular Ba^{++} (Fig. 1e). Bath application of MPD (100 mM) increased the amplitude of the inwardly rectifying current (Fig. 1e), indicating that MPD activates GIRK channels. Note also that MPD appeared to inhibit an endogenous voltage-gated outward current at positive potentials (Fig. 1e, arrow), which is likely a voltage-gated K channel9. All three alcohols activated GIRK2 channels at 10 mM and displayed a steep increase in activation around 100 mM (Fig. 2a). The activation curve for MPD falls between EtOH and 1-PrOH (Fig. 2b) and does not reach a maximum, similar to previous studies7,8. These results show that MPD activates GIRK2 in a similar manner to other small n-alcohols. Interestingly, 1-pentanol (1-PeOH), which also has five backbone carbons like MPD, predominantly inhibits GIRK2 channels (see Supplemental **Fig. S1**). Therefore, a large diol, such as MPD, activates GIRK2 channels in a similar manner to small primary alcohols, such as ethanol, but is different from 1-PeOH (see Discussion).

Pertussis toxin treatment does not prevent EtOH activation of GIRK channels, indicating that GPCR coupling to G proteins is not involved8. To rule out the possibility that alcohols activate GIRK channels by directly stimulating G protein heterotrimers and liberating Gβγ subunits, we measured the alcohol response of GIRK2 channels in cells co-expressing a myristoylated form of phosducin (m-Phos) that chelates Gβγ following stimulation of GPCRs26. Compared to controls, carbachol application led to smaller and rapidly desensitizing m2R evoked GIRK2 currents in cells coexpressing m-Phos (Fig. 2c–e). All three alcohols, on the other hand, activated GIRK2 channels to the same extent in the presence of m-Phos (Fig. 2d,e). Thus, alcohol-dependent activation of GIRK2 channels does

not appear to require free Gβγ subunits. Together, these results support the interpretation that alcohols directly activate GIRK channels through a physical alcohol-bound pocket.

Role for hydrophobic pocket in alcohol activation

To determine whether the hydrophobic pocket in GIRK2 mediates alcohol activation, we examined the effects of the side-chain volume using an amino acid with a small (Ala) or large (Trp) side-chain (Fig. 3a,b). Six mutants did not express basal K^+ currents (< −1 $pApF^{-1}$) (Fig. 3b). In mutant channels engineered with an extracellular hemagglutinin (HA)-tag, we investigated whether the lack of basal current was due to a trafficking defect using confocal microscopy. Four mutants, HA-GIRK2-Y58W, HA-GIRK2-Y58A, HA-GIRK2-L342W and HA-GIRK2-Y349A, expressed on the plasma membrane but did not conduct currents (Fig. 3b; Supplementary **Fig. S2**). Mutations at GIRK2-I244 impaired expression on the membrane surface (Fig. 3b). These findings suggest the hydrophobic pocket in GIRK2 is important for channel gating and/or assembly in the absence of alcohol. Four other mutants, GIRK2-L257A, GIRK2-L257W, GIRK2-L342A and GIRK2-Y349W, produced functional channels that were activated by EtOH (Fig. 3c). However, GIRK2-L257W displayed significantly smaller EtOH-activated currents (Fig. 3c), suggesting that Leu at position 257 in the βD-βE ribbon is a key residue that is required for alcohol-dependent activation of GIRK2 channels.

In the IRK1-MPD structure, L245, which is homologous to L257, is positioned at the base of the pocket, and interacts intimately with MPD. The decrease in EtOH-activated current of GIRK2-L257W raised the possibility that amino acids with bulky side-chains might generally interfere with alcohol activation. We systematically evaluated the effect of substituting twelve different amino acids of increasing molecular side-chain volume in GIRK2-L257. Of the twelve, five expressed (> −1 $pApF^{-1}$) and could be investigated further for possible changes in alcohol-mediated activation (Fig. 4a). The magnitude and rank order (1-PrOH > MPD > EtOH) for alcohol activation with smaller molecular volume substitutions, such as Ala, Cys and Met, were indistinguishable from wild-type Leu in GIRK2 channels (Figs. 4b,c and 5a). On the other hand, GIRK2-L257Y reduced 1-PrOH and MPD but not EtOH activation while GIRK2-L257W affected EtOH, 1-PrOH and MPD dependent activation (Figs. 4d,e and 5a). Interestingly, 100 mM MPD no longer activated and now inhibited the basal currents for GIRK2-L257W (Figs. 4e and 5a). For GIRK2-L257Y and GIRK2-L257W, the decrease in alcohol activation was observed at a full range of concentrations (25, 125, 250 mM) for 1-PrOH or MPD (Fig. 5b), indicating a significant impairment in alcohol sensitivity. In addition to the change in alcohol response, mutations at L257 also reduced the m2R-mediated currents (Figs. 4c-e and 5a), indicating that L257 is involved in both alcohol-mediated and Gβγ-mediated activation (see Discussion). Taken together, these results demonstrate that increasing the side-chain volume at L257 leads to a progressive loss in alcohol-mediated activation (Fig. 5a and **inset**). A switch in alcohol activation occurred with an increase in volume from wild-type Leu (101 $Å^3$) to Tyr (133 $Å^3$) or Trp (168 $Å^3$). In addition, bulky substitutions at L257 affected larger alcohols (MPD) more than smaller alcohols (EtOH), suggesting the molecular volume of the pocket is an important determinant of alcohol specificity.

Because alcohol activation is a property of most types of GIRK channels7,8, we reasoned that a homologous mutation in a related GIRK channel would also alter the response to alcohols. To test this idea, we investigated the effects of mutating L252 in GIRK4*. GIRK4* contains a mutation in the pore-helix (S143T) that enhances channel activity without affecting surface expression27. Substituting Ala (26 $Å^3$), Tyr (133 $Å^3$) or Trp (168 $Å^3$) at L252 in GIRK4* channels did not change the basal K^+ currents (Fig. 6a). Similar to mutations of L257 in GIRK2, Trp and Tyr substitutions in GIRK4* decreased EtOH, 1-PrOH and MPD activation, as compared to L252A, with 1-PrOH now inhibiting GIRK4*-L252W (Fig. 6b–f). In contrast to GIRK2, however, MPD activation of GIRK4*-L252W was not significantly different from wild-type (Fig. 6e,f). Mutating GIRK4*-L252 also significantly reduced m2R-activated GIRK currents (Fig. 6c–f). Thus, the putative hydrophobic alcohol-binding pocket in GIRK4* is important for mediating alcohol activation but GIRK4* may accommodate MPD differently than GIRK2 (see Discussion).

Mutations of MPD pocket do not alter alcohol inhibition

MPD is bound to a hydrophobic pocket in the crystal structure of IRK1, suggesting that MPD might inhibit IRK1 channels like other alcohols7,8. Bath applying 100 mM MPD inhibited nearly 50% the basal inwardly rectifying K^+ current through IRK1 channels (Fig. 7a). The MPD inhibition was dose dependent and had an IC_{50} of 104 ± 23 mM and a Hill coefficient of 0.93 ± 0.02 (n=8) (Fig. 7b). We next investigated whether Trp substitutions in the hydrophobic alcohol-binding pocket of IRK1 altered alcohol-dependent inhibition (Fig. 7c). IRK1-F47W, IRK1-L232W, IRK1-L245W IRK1-L330W but not IRK1-Y337W produced significant basal K^+ current (data not shown). Like wild-type IRK1, MPD inhibited the basal currents of mutant channels in a dose-dependent manner. In fact, the IC_{50} for MPD inhibition was indistinguishable among the different IRK1 mutants (Fig. 7d). Furthermore, IRK1-L245W mutation did not alter inhibition by EtOH, 1-PrOH or 1-BuOH (data not shown). Thus, mutations at the hydrophobic pocket of IRK1 channels do not appear to alter the sensitivity to inhibition by alcohols.

IRK1 channels are constitutively open, producing a large basal K^+ current. We speculated that alcohols might therefore inhibit GIRK channels engineered to be constitutively open. We introduced a high affinity PIP_2 site shown previously to produce a large basal current28,29 (GIRK2-PIP_2). In contrast to wild-type GIRK2, GIRK2-PIP_2 exhibited large basal currents as expected (−530 ± 197 $pApF^{-1}$, n=5). Application of 100 mM MPD inhibited the basal K^+ current of GIRK2-PIP_2 (Fig. 7e). Similar to IRK1, we hypothesized that mutating L257 to Trp in GIRK2-PIP_2 would have no effect in alcohol-mediated inhibition. Accordingly, GIRK2-PIP_2-L257W produced large Ba^{++}-sensitive currents (−363 ± 182 $pApF^{-1}$, n=6) that were inhibited by MPD, similar to GIRK2-PIP_2 channels (Fig. 7f). We conclude that the hydrophobic alcohol-binding pocket in IRK1 or GIRK2 is not involved in alcohol-dependent inhibition. Furthermore, these results show that constitutively open inwardly rectifying K^+ channels are not activated further by alcohols.

While investigating alcohol modulation of GIRK4*, we discovered that 1-BuOH activated GIRK4*, in contrast to inhibition of GIRK4 wild-type (Supplementary **Fig. S3**) or GIRK1/4 heterotetramers7,8. GIRK4 and GIRK4* differ by a point mutation (S143T) in the pore-

helix27 suggesting that S143T may regulate sensitivity to alcohol inhibition. To assess whether this site is generally involved in alcohol-mediated inhibition of GIRK channels, we introduced a Thr at the equivalent Ser (S148T) in GIRK2-PIP_2 channels. As predicted, GIRK2-PIP_2-S148T significantly shifted the IC_{50} for MPD-dependent inhibition compared to GIRK2-PIP_2 (Fig. 7f). Taken together, these experiments implicate amino acids in the pore-helix in regulating the extent of alcohol-dependent inhibition and support the conclusion that the cytoplasmic alcohol-binding pocket mediates alcohol-dependent activation, but not inhibition, of GIRK channels.

Discussion

Based on high-resolution channel structures and functional mutagenesis, we have identified a physical site for alcohol-mediated activation of GIRK channels. Amino acid substitutions that increased the molecular side-chain volume at a conserved Leu in the βD-βE ribbon of the hydrophobic pocket of GIRK2 decreased alcohol-mediated activation of GIRK channels (see Fig. 8a). In particular, two substitutions, Trp and Tyr, at the Leu in the hydrophobic pocket of GIRK2 (L257) and GIRK4* (L252) channels produced a progressive loss in alcohol activation. For GIRK4*, Ala substitution increased the amplitude of alcohol-activated currents. Thus, increasing or decreasing the volume of the pocket by altering the amino acid side-chain produced changes in alcohol activation. Similarly, the size of the putative alcohol-binding pocket in $GABA_A$ α1 and glycine receptors is important for determining modulation by alcohol and other small anesthetics. Increasing the bulkiness of amino acids in the putative alcohol-binding pocket of these channels eliminates the modulation by EtOH3 or isofluorane30. By contrast, decreasing the size of amino acids in the same region of the decanol-*insensitive* GABA ρ1 receptors now enables potentiation by decanol3,6. Taken together with our findings, these studies support a model that physical pockets of defined dimensions can be probed with mutations that change the dimension of the alcohol-binding sites. Using the IRK1-MPD structure as a guide, we estimate the volume of the hydrophobic alcohol binding pocket of GIRK channels to be ∼250 $Å^3$, which is large enough to accommodate bulky alcohols like MPD (∼130 $Å^3$, Fig. 8b). A Trp mutation in the pocket would decrease the volume that could potentially occlude larger alcohols (Fig. 8b). In addition, the sensitivity to activation may be different between GIRK2 and GIRK4* channels. For example, Trp substitution in GIRK2 eliminated MPD activation, revealing inhibition of current. In GIRK4*, Trp substitution eliminated 1-PrOH activation but showed only a significant decrease in MPD activation when comparing Ala with Trp substitutions. One possible explanation is that MPD fits differently in the alcohol pocket of GIRK4*, which could be revealed in a complex of MPD and GIRK4 structure.

The observations that mutations at the hydrophobic pocket did not alter alcohol-dependent inhibition of IRK1, and that S148T mutation (but not L257W) in GIRK2-PIP_2 decreased alcohol-dependent inhibition suggest that GIRK channels possess two different sites for alcohol modulation. In the Kirbac1.3 structure, the Ser is located in the pore helix of Kirbac1.3 where there is no space for alcohol (Supplemental **Fig. S4**), suggesting that S148 regulates the sensitivity to inhibition but does not form the binding site. Alcohols might interfere with ion permeation or possibly with gating at the transmembrane domains, similar to voltage-gated K channels9. Another possibility is that alcohols inhibit the channel by

altering the fluidity of the lipid membrane5 and/or decreasing interactions with phospholipid phosphatidylinositol bisphosphate (PIP_2), which is required for channel function31.

Interestingly, whereas 1-octanol inhibits GIRK channels, co-application of 1-octanol with EtOH has no effect on EtOH-mediated activation, also raising the possibility of a second site for inhibition7. The net effect of alcohol modulation in GIRK channels would therefore be determined by the relative potencies of activation and inhibition. In support of this, we found that bath application of 1-PeOH inhibited GIRK2 channels but induced a large current immediately after washout (Supplementary **Fig. S1**), revealing two components of alcohol modulation. It is notable that MPD predominantly activates GIRK channels in contrast to large primary alcohol of similar size. A functional difference between diols and primary alcohols has been reported previously for NMDA channels32. The addition of a hydroxyl group may lead to decreased sensitivity to inhibition for GIRK channels. The presence of two sites for alcohol modulation also suggests that ascribing a cutoff number for alcohol activation of GIRK channels would not be accurate, in contrast to the determination of the cutoff number for $GABA_A$ channels33.

Two different types of alcohol-bound protein structures have been solved previously, the enzymatic/catalytic alcohol dehydrogenase (ADH) and a non-catalytic Drosophila odorant-binding protein, LUSH. In ADH, primary alcohol is coordinated with Zn^{2+} in a hydrophobic pocket, where it catalyzes the oxidation of alcohol to aldehyde34,35. Mutagenesis studies in the pocket indicated the bulkiness of side-chains in the hydrophobic pocket determines alcohol specificity36. The high-resolution structure of LUSH in complex with small alcohols showed that in addition to hydrophobic interactions, a network of hydrogen bonds help stabilize alcohol in the LUSH alcohol-binding pocket22,37. The hydrophobic pocket in IRK1-MPD has many of the same features of these alcohol-binding pockets. First, hydrophobic amino acids form the pocket and interact intimately with hydrocarbons of the alcohol (Fig. 1b). In GIRK2, mutations of L257 to bulkier amino acids significantly reduced or eliminated alcohol-mediated activation. This finding is consistent with the role of hydrophobic side-chains in determining the size of the alcohol-binding pocket. Second, the IRK1-MPD structure indicates that hydrogen-bonds form between MPD and the backbone carbonyl of P244, Y242 via a water and a hydroxyl of Y337 (Fig. 1)21. At the homologous position for IRK1-Y242, GIRK2 contains a Phe (F254), which indicates that this hydrogen-bond triangle may not be essential. Additionally, we found that MPD-mediated activation was not affected by Y349W mutation at the homologous position of IRK1-Y337) (Supplemental **Fig. S5**). Therefore, it is possible that the carbonyl group of Pro in the βD-βE ribbon is the linchpin that stabilizes alcohol in the pocket via hydrogen-bonding. Unnatural amino acid mutagenesis38 would be needed to further establish the importance of this hydrogen-bond interaction in stabilizing alcohol.

Though specific alcohol-induced conformational changes in the channel protein remain to be determined, our structural analysis between IRK1-MPD structure and that of chimeric KirBac1.3-GIRK1 structure provides some new clues into channel gating24,39. Two different conformational states of GIRK have been described: a putative open state, due to the open position of the G-loops in the cytoplasmic gate24,39 (GIRK1-*open*, Fig. 8c) and a putative closed state (GIRK1-*closed*, Fig. 8c). We aligned the IRK1-MPD structure with

these two different Kirbac1.3-GIRK1 structures, and discovered that IRK1-MPD structure aligns better with the GIRK1-*open* in the hydrophobic alcohol-binding pocket (Fig. 8c, **zoom**). By contrast, the alignment with GIRK1-*closed* structure shows striking differences in the hydrophobic alcohol pocket. In particular, the side-chains from F46 in the N-terminal domain, L246 in the βD-βE ribbon and L333 in the βL-βM ribbon fill the hydrophobic pocket of the putative closed state of GIRK1. In the open state, however, structural rearrangements of F46, L246, L333 and F338 occur that enable MPD to now fit in the pocket.

Based on our mutagenesis data and structural analyses, we propose a tenable model for alcohol activation of GIRK channels. At rest, GIRK2 channels undergo infrequent structural rearrangements in the pocket that correlate with the open and closed positions of the channel's cytoplasmic gates, the G loops24,39 and M2 transmembrane domains40-42 (Fig. 8c). Alcohol entering the pocket could then stabilize the open conformation, leading to alcohol-activated currents. Bulky substitutions at L257/L252 of GIRK channels, located at the base of the alcohol pocket, would hinder alcohols from filling the pocket. Alcohols might also displace other amino acids that fill the hydrophobic pocket in the closed state (Fig. 8c), promoting the open state. Previous studies have suggested that Gβγ-dependent activation of GIRK channels involves increases in PIP_2 affinity28,31. Similarly, changes in PIP_2 binding may also be involved in alcohol-dependent activation of GIRK channels. Studies in the future will need to investigate the molecular relationships between movement of the N-terminal domain, βD-βE and βL-βM ribbons within the hydrophobic pocket, PIP_2 interactions, and the channel gates.

The alcohol-binding pocket may also be involved in Gβγ-dependent activation. Mutation of a conserved Leu (GIRK2-L344, GIRK4*L339, GIRK1-L333, Fig. 8c) to Glu in the βL-βM ribbon of GIRK channels attenuates Gβγ activation17-19. We found that mutations in the βD-βE (L257) ribbon that altered alcohol-dependent activation also reduced Gβγ-dependent activation (Figs. 4 and 5). Together, these results suggest that conformational changes in the βD-βE and βL-βM structural elements, along with the N-terminal domain43,44, may be central to both alcohol-and Gβγ-dependent activation. Intriguingly, hydrophobic amino acids in the G protein Gβ subunit have been implicated in GIRK channel activation45, which perhaps interact directly with the alcohol-binding pocket in GIRK.

Materials and Methods

Molecular Biology and Cell Culture

cDNAs for mouse GIRK2c46 (GIRK2c is referred to as ‘GIRK2’ in this study for clarity), rat GIRK4[Krapivinsky, 1998 #126], mouse IRK124, human m2R46, and bovine m-Phos26 were subcloned into pcDNA3.1 vector (Invitrogen). GIRK4* contains a S143T mutation in the pore-helix27. Point mutations were introduced by Quickchange site directed mutagenesis kit (Stratagene). GIRK2-PIP_2 mutant was created by overlap-PCR method47. Briefly, a region of GIRK2-D228-L234 was replaced with the homologous region of IRK1-N216-L222; this region contains seven amino acids in the βC-βD region implicated previously in PIP_2 binding28,29 (we refer to this mutant as GIRK2-PIP_2). All mutations were confirmed by DNA sequencing. HEK-293T cells were cultured in DMEM supplemented with 10%

fetal bovine serum, and 1X Glutamax (Invitrogen) in a humidified 37° C incubator with 5% CO_2. Cells were plated in 12 well dish, and transiently transfected with DNA using Lipofectamine 2000 (Invitrogen). Cells were replated to 12-mm glass coverslips coated with poly-D-Lysine (20 μg/ml) 12−24 hr after transfection.

Detection of channels expressed on membrane surface

GIRK2c and mutant channels were engineered with an extracellular hemagglutinin (HA) epitope inserted between I126 - E127 for immunohistochemical detection with anti-HA antibodies46. HEK-293T cells were transfected with 0.5 μg of channel cDNA and examined 24−48 hr after transfection. Cells were washed with 1X Dulbecco's Phosphate Buffer Saline (DPBS; Invitrogen), fixed with 2% para-formaldehyde (PFA) in 1X DPBS for 10 min and rinsed with 1X DPBS (at 22−25° C). To label surface channels, cells were incubated with blocking buffer (3% BSA in 1X DPBS) for 1 hr and then with anti-HA mouse antibody (1:400 in blocking buffer; Covance) for 2 hr at 22° C. To label cytoplasmic channels, cells were rinsed with 1X DPBS, permeabilized with 0.25% TritonX-100 (Sigma) in blocking buffer for 10 min at 22° C and incubated with blocking buffer for 1 hr. Cells were then incubated with rabbit anti-GIRK2 (1:200 in blocking buffer; Alomone) for 2 hrs. Following rinses in 1X DPBS, cells were incubated with fluorescent secondary antibodies, anti-mouse Alexa-647 and anti-rabbit Alexa-488 (1:300; Invitrogen) for 1 hr in the dark. Cells were rinsed with 1X DPBS, mounted on microscope slides using Progold anti-fading reagent (Invitrogen), and both fluorophores imaged with a Leica TSC SP2 AOBS laser confocal microscope.

Whole-cell patch-clamp electrophysiology

HEK-293T cells were transfected with 0.2 μg of channel cDNA and 0.04 μg of eYFP cDNA to identify transfected cells. For some experiments, 0.8 μg of m2R and 0.8 μg of m-Phos cDNA were also transfected. Whole-cell patch clamp recordings were performed 24−72 hr after transfection. Borosilicate glass electrodes (Warner Instruments) of 5−7 mΩ were filled with intracellular solution (130 mM KCl, 20 mM NaCl, 5 mM EGTA, 2.56 mM K_2ATP, 5.46 mM $MgCl_2$, 0.30 mM Li_2GTP, and 10 mM HEPES, pH 7.4). Extracellular 20K solution contained 20mM KCl, 140mM NaCl, 0.5mM $CaCl_2$, 2mM $MgCl_2$ and 10mM HEPES (pH7.4). Alcohols (0.1 − 300 mM), carbachol (5 μM), or $BaCl_2$ (1 mM) were diluted into the 20K solution and applied directly to the cell with the rapid valve-controlled, perfusion system (Warner Instruments, VC6, MM-6 manifold). All chemicals for electrophysiology were purchased from Sigma-Aldrich. Whole-cell patch-clamp currents were recorded using Axopatch 200B (Molecular Devices; Axon Instruments) amplifier. Currents were adjusted electronically for cell capacitance and series resistance (80−100%), filtered at 1kHz with an 8-pole Bessel filter and digitized at 5kHz with a Digidata 1200 interface (Molecular Devices: Axon Instruments). Currents were elicited with voltage ramp protocol, from −100 mV to +50 mV, delivered at 0.5 Hz. Currents were measured at −100 mV and converted to current density ($pApF^{-1}$) by dividing by the membrane capacitance. Basal K^+ currents (Ba^{++}-sensitive) were quantified at −100 mV by applying 1 mM $BaCl_2$ in 20K and measuring the amplitude of the Ba^{++}-inhibited current. Alcohol- and carbachol-modulated currents were measured at −100 mV by averaging current from two consecutive sweeps upon reaching steady state, and subtracting the mean basal current before and after

the application of the modulator. Pooled data are presented as mean ± s.e.m. and evaluated for statistical significance ($P < 0.05$) using a one-way ANOVA, followed by Bonferroni multiple comparison post-hoc test. To determine the $IC_{50,}$ the inhibition curves were fit with the Hill equation y=1/(1+[x/c]^b), where y is fraction current remaining, x is the concentration of alcohol, b is the Hill coefficient and c is the IC_{50}, the concentration of alcohol that produces 50% inhibition48.

Structural Analysis

Molecular representations were made using PyMOL (DeLano Scientific) with PDB files 2GIX (IRK1-MPD), 2E4F(GIRK2) and 2QKS (Kirbac1.3-GIRK1). The cavity of the IRK1-MPD pocket was calculated using CASTp server49 with 1.4 Å probe radius. L245W was modeled in the IRK1-MPD structure by optimizing the best rotamer position for Trp using PyMOL software. Molecular volume estimates for amino acid side-chains were based on reported values50.

Supplementary Material

Refer to Web version on PubMed Central for supplementary material.

Acknowledgements

We would like to thank Y. Kurachi for GIRK2 (PDB: 2E4F) coordinates, M. Lazdunsky for GIRK2 cDNA, D. Clapham for GIRK4 cDNA N. Dascal for m-Phos cDNA, S. Pegan for initial discussions on structure of IRK1-MPD (PDB: 2GIX) and members of the Slesinger lab for helpful comments. This work was funded, in part, by a pre-doctoral NIH NRSA fellowship to P.A. (Award Number F31AA017042) from the National Institute on Alcohol Abuse and Alcoholism, the H. N. & Frances C. Berger Foundation, and the Salk Institute for Biological Studies. The content is solely the responsibility of the authors and does not necessarily represent the official views of the National Institute on Alcohol Abuse and Alcoholism or the National Institutes of Health.

References

1. Cardoso RA, Brozowski SJ, Chavez-Noriega LE, Harpold M, Valenzuela CF, Harris RA. Effects of ethanol on recombinant human neuronal nicotinic acetylcholine receptors expressed in Xenopus oocytes. J Pharmacol Exp Ther. 1999; 289:774–780. [PubMed: 10215652]
2. Lovinger DM, White G, Weight FF. Ethanol inhibits NMDA-activated ion current in hippocampal neurons. Science. 1989; 243:1721–1724. [PubMed: 2467382]
3. Mihic SJ, Ye Q, Wick MJ, Koltchine VV, Krasowski MD, Finn SE, Mascia MP, Valenzuela CF, Hanson KK, Greenblatt EP, Harris RA, Harrison NL. Sites of alcohol and volatile anaesthetic action on $GABA_A$ and glycine receptors. Nature. 1997; 389:385–389. [PubMed: 9311780]
4. Zhou Q, Lovinger DM. Pharmacologic characteristics of potentiation of 5-HT3 receptors by alcohols and diethyl ether in NCB-20 neuroblastoma cells. J Pharmacol Exp Ther. 1996; 278:732–740. [PubMed: 8768725]
5. Harris RA, Trudell JR, Mihic SJ. Ethanol's molecular targets. Sci Signal. 2008; 1:re7. [PubMed: 18632551]
6. Wick MJ, Mihic SJ, Ueno S, Mascia MP, Trudell JR, Brozowski SJ, Ye Q, Harrison NL, Harris RA. Mutations of gamma-aminobutyric acid and glycine receptors change alcohol cutoff: evidence for an alcohol receptor? Proc Natl Acad Sci U S A. 1998; 95:6504–6509. [PubMed: 9600996]
7. Lewohl JM, Wilson WR, Mayfield RD, Brozowski SJ, Morrisett RA, Harris RA. G-protein-coupled inwardly rectifying potassium channels are targets of alcohol action. Nat Neurosci. 1999; 2:1084–1090. [PubMed: 10570485]

8. Kobayashi T, Ikeda K, Kojima H, Niki H, Yano R, Yoshioka T, Kumanishi T. Ethanol opens G-protein-activated inwardly rectifying K^+ channels. Nat Neurosci. 1999; 2:1091–1097. [PubMed: 10570486]

9. Covarrubias M, Vyas TB, Escobar L, Wei A. Alcohols inhibit a cloned potassium channel at a discrete saturable site. Insights into the molecular basis of general anesthesia. J Biol Chem. 1995; 270:19408–19416. [PubMed: 7642622]

10. Blednov YA, Stoffel M, Alva H, Harris RA. A pervasive mechanism for analgesia: activation of GIRK2 channels. Proc Natl Acad Sci U S A. 2003; 100:277–282. [PubMed: 12493843]

11. Blednov YA, Stoffel M, Chang SR, Harris RA. Potassium channels as targets for ethanol: studies of G-protein-coupled inwardly rectifying potassium channel 2 (GIRK2) null mutant mice. J Pharmacol Exp Ther. 2001; 298:521–530. [PubMed: 11454913]

12. Reuveny E, Slesinger PA, Inglese J, Morales JM, Iniguez-Lluhi JA, Lefkowitz RJ, Bourne HR, Jan YN, Jan LY. Activation of the cloned muscarinic potassium channel by G protein βγ subunits. Nature. 1994; 370:143–146. [PubMed: 8022483]

13. Wickman KD, Iniguez-Lluhl JA, Davenport PA, Taussig R, Krapivinsky GB, Linder ME, Gilman AG, Clapham DE. Recombinant G-protein βγ-subunits activate the muscarinic-gated atrial potassium channel. Nature. 1994; 368:255–257. [PubMed: 8145826]

14. Huang CL, Slesinger PA, Casey PJ, Jan YN, Jan LY. Evidence that direct binding of G βγ to the GIRK1 G protein-gated inwardly rectifying K^+ channel is important for channel activation. Neuron. 1995; 15:1133–1143. [PubMed: 7576656]

15. Kunkel MT, Peralta EG. Identification of domains conferring G protein regulation on inward rectifier potassium channels. Cell. 1995; 83:443–449. [PubMed: 8521474]

16. Krapivinsky G, Kennedy ME, Nemec J, Medina I, Krapivinsky L, Clapham DE. Gβγ binding to GIRK4 subunit is critical for G protein-gated K^+ channel activation. J Biol Chem. 1998; 273:16946–16952. [PubMed: 9642257]

17. He C, Zhang H, Mirshahi T, Logothetis DE. Identification of a potassium channel site that interacts with G protein βγ subunits to mediate agonist-induced signaling. J Biol Chem. 1999; 274:12517–12524. [PubMed: 10212228]

18. Ivanina T, Rishal I, Varon D, Mullner C, Frohnwieser-Steinecke B, Schreibmayer W, Dessauer CW, Dascal N. Mapping the Gβγ-binding sites in GIRK1 and GIRK2 subunits of the G protein-activated K^+ channel. J Biol Chem. 2003; 278:29174–29183. [PubMed: 12743112]

19. Finley M, Arrabit C, Fowler C, Suen KF, Slesinger PA. βL-βM loop in the C-terminal domain of G protein-activated inwardly rectifying K^+ channels is important for G(βγ) subunit activation. J Physiol. 2004; 555:643–657. [PubMed: 14724209]

20. Hara K, Lewohl JM, Yamakura T, Harris RA. Mutational analysis of ethanol interactions with G-protein-coupled inwardly rectifying potassium channels. Alcohol. 2001; 24:5–8. [PubMed: 11524176]

21. Pegan S, Arrabit C, Slesinger PA, Choe S. Andersen's syndrome mutation effects on the structure and assembly of the cytoplasmic domains of Kir2.1. Biochemistry. 2006; 45:8599–8606. [PubMed: 16834334]

22. Kruse SW, Zhao R, Smith DP, Jones DN. Structure of a specific alcohol-binding site defined by the odorant binding protein LUSH from Drosophila melanogaster. Nat Struct Biol. 2003; 10:694–700. [PubMed: 12881720]

23. Nishida M, MacKinnon R. Structural basis of inward rectification: cytoplasmic pore of the G protein-gated inward rectifier GIRK1 at 1.8 Å resolution. Cell. 2002; 111:957–965. [PubMed: 12507423]

24. Pegan S, Arrabit C, Zhou W, Kwiatkowski W, Collins A, Slesinger PA, Choe S. Cytoplasmic domain structures of Kir2.1 and Kir3.1 show sites for modulating gating and rectification. Nat Neurosci. 2005; 8:279–287. [PubMed: 15723059]

25. Inanobe A, Matsuura T, Nakagawa A, Kurachi Y. Structural Diversity in the Cytoplasmic Region of G Protein-Gated Inward Rectifier K^+ Channels. Channels (Austin). 2007; 1:39–45. [PubMed: 19151589]

26. Rishal I, Porozov Y, Yakubovich D, Varon D, Dascal N. Gβγ -dependent and Gβγ-independent basal activity of G protein-activated K^+ channels. J Biol Chem. 2005; 280:16685–16694. [PubMed: 15728579]
27. Vivaudou M, Chan KW, Sui JL, Jan LY, Reuveny E, Logothetis DE. Probing the G-protein regulation of GIRK1 and GIRK4, the two subunits of the KACh channel, using functional homomeric mutants. J Biol Chem. 1997; 272:31553–31560. [PubMed: 9395492]
28. Zhang H, He C, Yan X, Mirshahi T, Logothetis DE. Activation of inwardly rectifying K^+ channels by distinct PtdIns(4,5)P2 interactions. Nat Cell Biol. 1999; 1:183–188. [PubMed: 10559906]
29. Zhou W, Arrabit C, Choe S, Slesinger PA. Mechanism underlying bupivacaine inhibition of G protein-gated inwardly rectifying K^+ channels. Proc Natl Acad Sci U S A. 2001; 98:6482–6487. [PubMed: 11353868]
30. Jenkins A, Greenblatt EP, Faulkner HJ, Bertaccini E, Light A, Lin A, Andreasen A, Viner A, Trudell JR, Harrison NL. Evidence for a common binding cavity for three general anesthetics within the $GABA_A$ receptor. J Neurosci. 2001; 21:RC136. [PubMed: 11245705]
31. Huang CL, Feng S, Hilgemann DW. Direct activation of inward rectifier potassium channels by PIP2 and its stabilization by Gβγ. Nature. 1998; 391:803–806. [PubMed: 9486652]
32. Peoples RW, Ren H. Inhibition of N-methyl-D-aspartate receptors by straight-chain diols: implications for the mechanism of the alcohol cutoff effect. Mol Pharmacol. 2002; 61:169–176. [PubMed: 11752218]
33. Dildy-Mayfield JE, Mihic SJ, Liu Y, Deitrich RA, Harris RA. Actions of long chain alcohols on $GABA_A$ and glutamate receptors: relation to in vivo effects. Br J Pharmacol. 1996; 118:378–384. [PubMed: 8735641]
34. Ramaswamy S, Eklund H, Plapp BV. Structures of horse liver alcohol dehydrogenase complexed with NAD+ and substituted benzyl alcohols. Biochemistry. 1994; 33:5230–5237. [PubMed: 8172897]
35. Svensson S, Hoog JO, Schneider G, Sandalova T. Crystal structures of mouse class II alcohol dehydrogenase reveal determinants of substrate specificity and catalytic efficiency. J Mol Biol. 2000; 302:441–453. [PubMed: 10970744]
36. Weinhold EG, Benner SA. Engineering yeast alcohol dehydrogenase. Replacing Trp54 by Leu broadens substrate specificity. Protein Eng. 1995; 8:457–461. [PubMed: 8532667]
37. Thode AB, Kruse SW, Nix JC, Jones DN. The role of multiple hydrogen-bonding groups in specific alcohol binding sites in proteins: insights from structural studies of LUSH. J Mol Biol. 2008; 376:1360–1376. [PubMed: 18234222]
38. Lu T, Ting AY, Mainland J, Jan LY, Schultz PG, Yang J. Probing ion permeation and gating in a K^+ channel with backbone mutations in the selectivity filter. Nat Neurosci. 2001; 4:239–246. [PubMed: 11224539]
39. Nishida M, Cadene M, Chait BT, MacKinnon R. Crystal structure of a Kir3.1-prokaryotic Kir channel chimera. EMBO J. 2007; 26:4005–4015. [PubMed: 17703190]
40. Yi BA, Lin YF, Jan YN, Jan LY. Yeast screen for constitutively active mutant G protein-activated potassium channels. Neuron. 2001; 29:657–667. [PubMed: 11301025]
41. Sadja R, Smadja K, Alagem N, Reuveny E. Coupling Gβγ -dependent activation to channel opening via pore elements in inwardly rectifying potassium channels. Neuron. 2001; 29:669–680. [PubMed: 11301026]
42. Jin T, Peng L, Mirshahi T, Rohacs T, Chan KW, Sanchez R, Logothetis DE. The βγ subunits of G proteins gate a K^+ channel by pivoted bending of a transmembrane segment. Mol Cell. 2002; 10:469–481. [PubMed: 12408817]
43. Sarac R, Hou P, Hurley KM, Hriciste D, Cohen NA, Nelson DJ. Mutation of critical GIRK subunit residues disrupts N- and C-termini association and channel function. J Neurosci. 2005; 25:1836–1846. [PubMed: 15716420]
44. Riven I, Kalmanzon E, Segev L, Reuveny E. Conformational rearrangements associated with the gating of the G protein-coupled potassium channel revealed by FRET microscopy. Neuron. 2003; 38:225–235. [PubMed: 12718857]

45. Ford CE, Skiba NP, Bae H, Daaka Y, Reuveny E, Shekter LR, Rosal R, Weng G, Yang C-S, Iyengar R, Miller RJ, Jan LY, Lefkowitz RJ, Hamm HE. Molecular basis for interactions of G protein βγ subunits with effectors. Science. 1998; 280:1271–1274. [PubMed: 9596582]

46. Clancy SM, Fowler CE, Finley M, Suen KF, Arrabit C, Berton F, Kosaza T, Casey PJ, Slesinger PA. Pertussis-toxin-sensitive Galpha subunits selectively bind to C-terminal domain of neuronal GIRK channels: evidence for a heterotrimeric G-protein-channel complex. Mol Cell Neurosci. 2005; 28:375–389. [PubMed: 15691717]

47. Ho SN, Hunt HD, Horton RM, Pullen JK, Pease LR. Site-directed mutagenesis by overlap extension using the polymerase chain reaction. Gene. 1989; 77:51–59. [PubMed: 2744487]

48. Kuo A, Gulbis JM, Antcliff JF, Rahman T, Lowe ED, Zimmer J, Cuthbertson J, Ashcroft FM, Ezaki T, Doyle DA. Crystal structure of the potassium channel KirBac1.1 in the closed state. Science. 2003; 300:1922–1926. [PubMed: 12738871]

49. Dundas J, Ouyang Z, Tseng J, Binkowski A, Turpaz Y, Liang J. CASTp: computed atlas of surface topography of proteins with structural and topographical mapping of functionally annotated residues. Nucleic Acids Res. 2006; 34:W116–118. [PubMed: 16844972]

50. Harpaz Y, Gerstein M, Chothia C. Volume changes on protein folding. Structure. 1994; 2:641–649. [PubMed: 7922041]

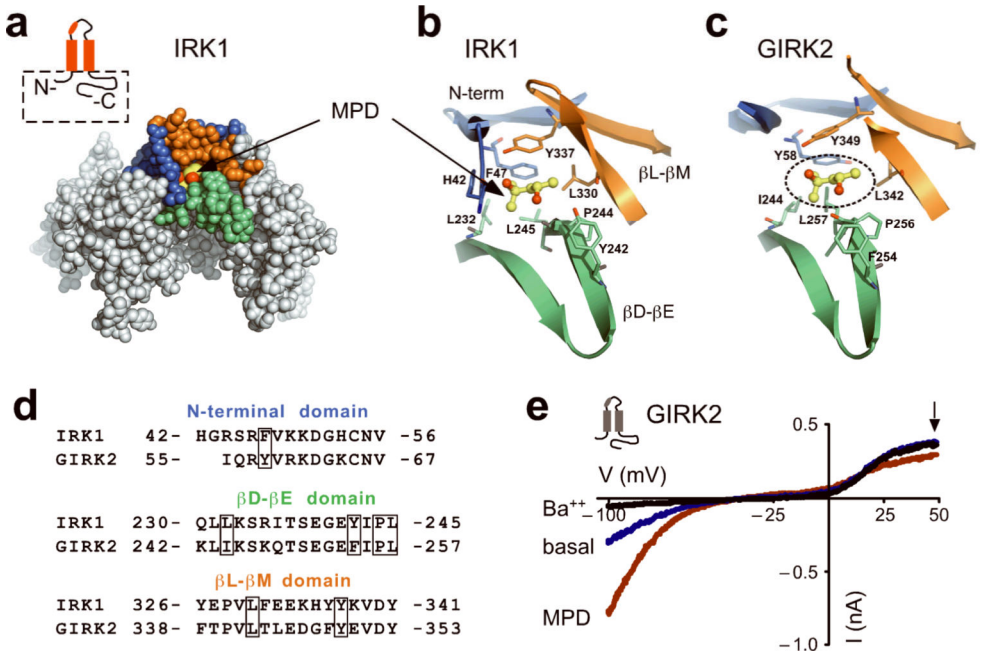

Fig. 1. A conserved alcohol-binding pocket in IRK1 and GIRK2 channels

a) CPK representation of the cytoplasmic domains from two subunits of IRK1 in complex with an alcohol, MPD (PDB: 2GIX). The pocket for MPD is formed by three structural elements: the N-terminal domain (blue) and the βL-βM ribbon (orange) from one subunit, and the βD-βE ribbon (green) from an adjacent subunit. Inset, schematic of IRK1 (red) shows the major structural elements of the subunit including pore loop and helix, two transmembrane domains, and N- and C-terminals used in the structure (dashed box). **b,c**) Detailed structural views of amino acids forming the hydrophobic alcohol pocket of IRK1 with MPD (ball and stick) (**b**) and a putative hydrophobic alcohol pocket in GIRK2 (PDB: 2E4F) (**c**). Amino acid residues shown in stick format are colored according to the domain they originate from; as MPD is shown in ball-and-stick format. The putative position of MPD in the GIRK2 (dashed circle) was obtained by superposition of two adjacent cytoplasmic domains from IRK1 structure and corresponding subunits from GIRK2 structure. **d**) Sequence alignment for the three domains comprising the hydrophobic alcohol pocket in IRK1 and GIRK2 channels. Boxes indicate amino acids that form hydrophobic and hydrogen-bond interactions in IRK1-MPD, and are conserved in GIRK2. 'HG' in the N-terminal domain of IRK1 originates from the polypeptide linker in the IRK1-MPD structure. **e**) Current-voltage plots for GIRK2 channels recorded in the presence of 20K (blue), 20K plus 1 mM Ba^{++} (black) or 20K plus 100 mM MPD (red). Currents were elicited by voltage ramps from −100 mV to +50 mV. MPD-induced current was 246% ± 27% (n=5, mean and s.e.m.) of basal K^+ current (Ba^{++} sensitive).

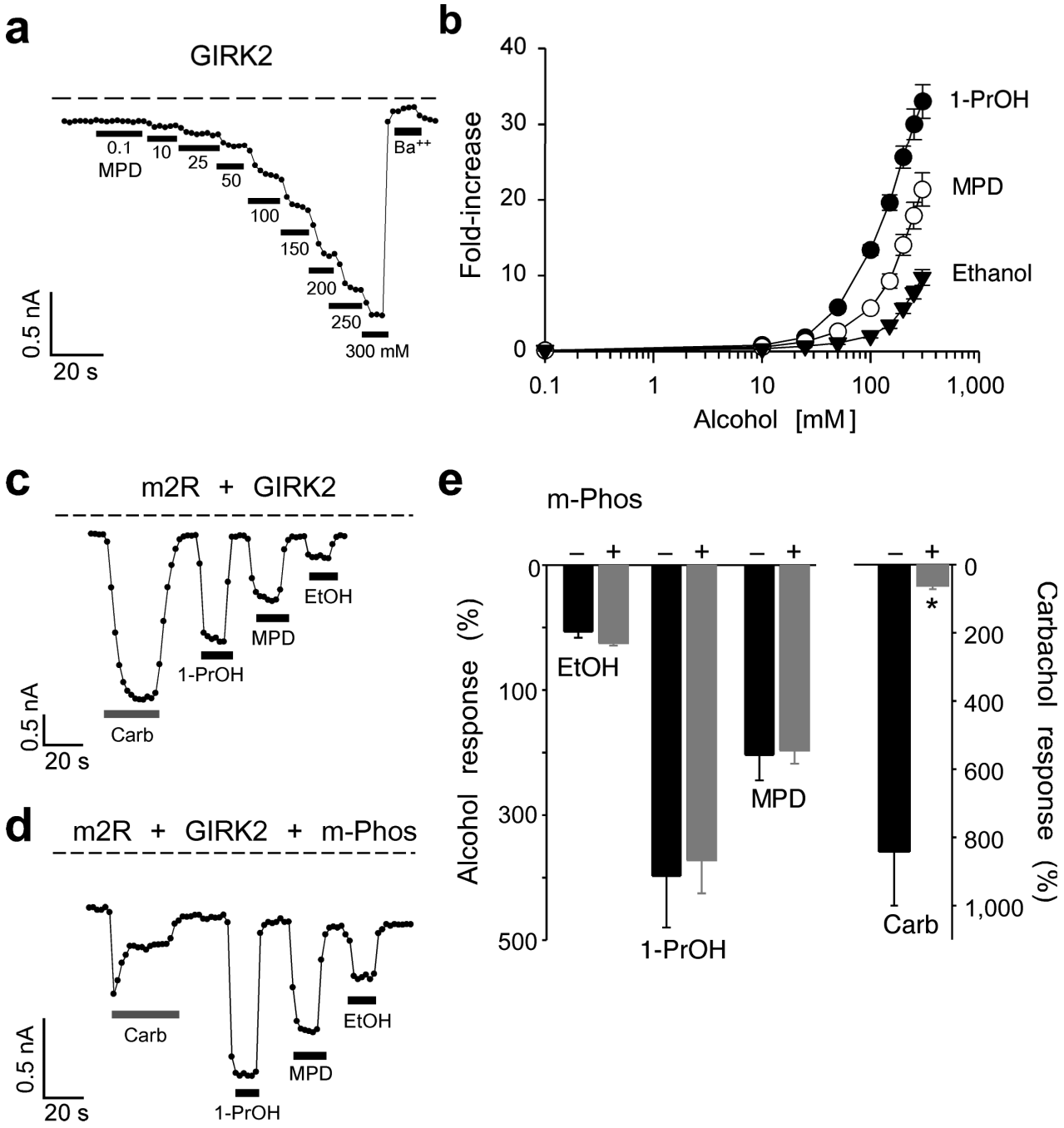

Fig. 2. MPD activates GIRK2 in a manner similar to other alcohols

a) The inward current through GIRK2 channels plotted as a function of time (at −100 mV) shows the response to the increasing concentrations of MPD and to 1 mM Ba^{++}. Dashed line shows zero current level. **b**) Dose-response curves are shown for MPD (n=6), 1-PrOH (n=6), and EtOH (n=6). The fold-increase was calculated by normalizing to the basal K^+ current (Ba^{++}-sensitive). **c-e**) Chelating Gβγ with m-Phos attenuates m2R- but not alcohol-mediated activation of GIRK2. Current responses recorded at −100 mV are shown for m2R/GIRK2 (**c**) or m2R/GIRK2/m-Phos (**d**) in response to 100 mM 1-PrOH, 100 mM MPD, 100 mM

EtOH, or 5 μM carbachol. **e**) Bar graphs show the mean percentage alcohol and carbachol responses (± s.e.m.), normalized to the Ba^{++}-sensitive basal current, in the absence (solid, n=4) or presence of m-Phos (grey, n=7). Asterisks indicate statistical significant difference from wild-type ($P < 0.05$).

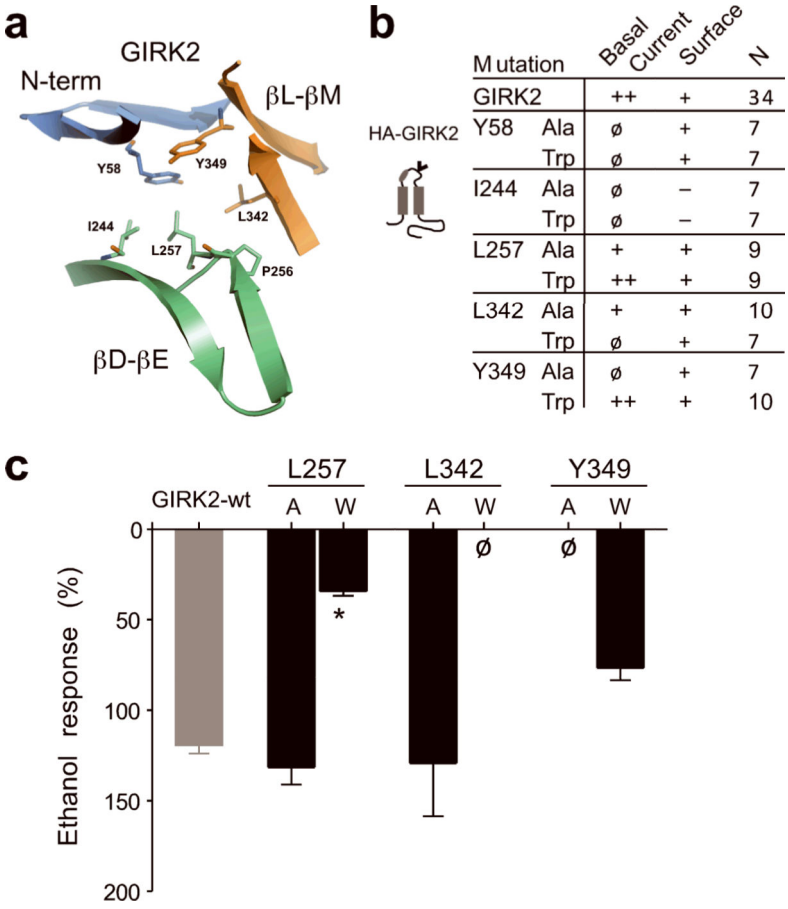

Fig. 3. Ala/Trp scan of the hydrophobic alcohol-binding pocket in GIRK2

a) Ribbon structure shows amino acids that line the hydrophobic alcohol pocket in GIRK2. **b**) Summary table of Ala/Trp mutagenesis. Basal K^+ currents (Ba^{++}-sensitive) were divided into three groups; < −1 $pApF^{-1}$ (ø), −1 to −5 $pApF^{-1}$ (+) and > −5 $pApF^{-1}$ (++) (n = number of recordings). Surface expression on the plasma membrane was assessed in separate experiments with HA-tagged channels; detected on the surface (+) or detected only in cytoplasm (−). See Supplemental **Fig. S1**. Schematic shows location of HA tag ('v') in GIRK2 (grey). **c)** Bar graph shows the mean ethanol percentage response, normalized to the basal K^+ current, for different mutant channels (± s.e.m.). L257W showed a significant statistical decrease in EtOH response (*P < 0.05 vs. wild-type).

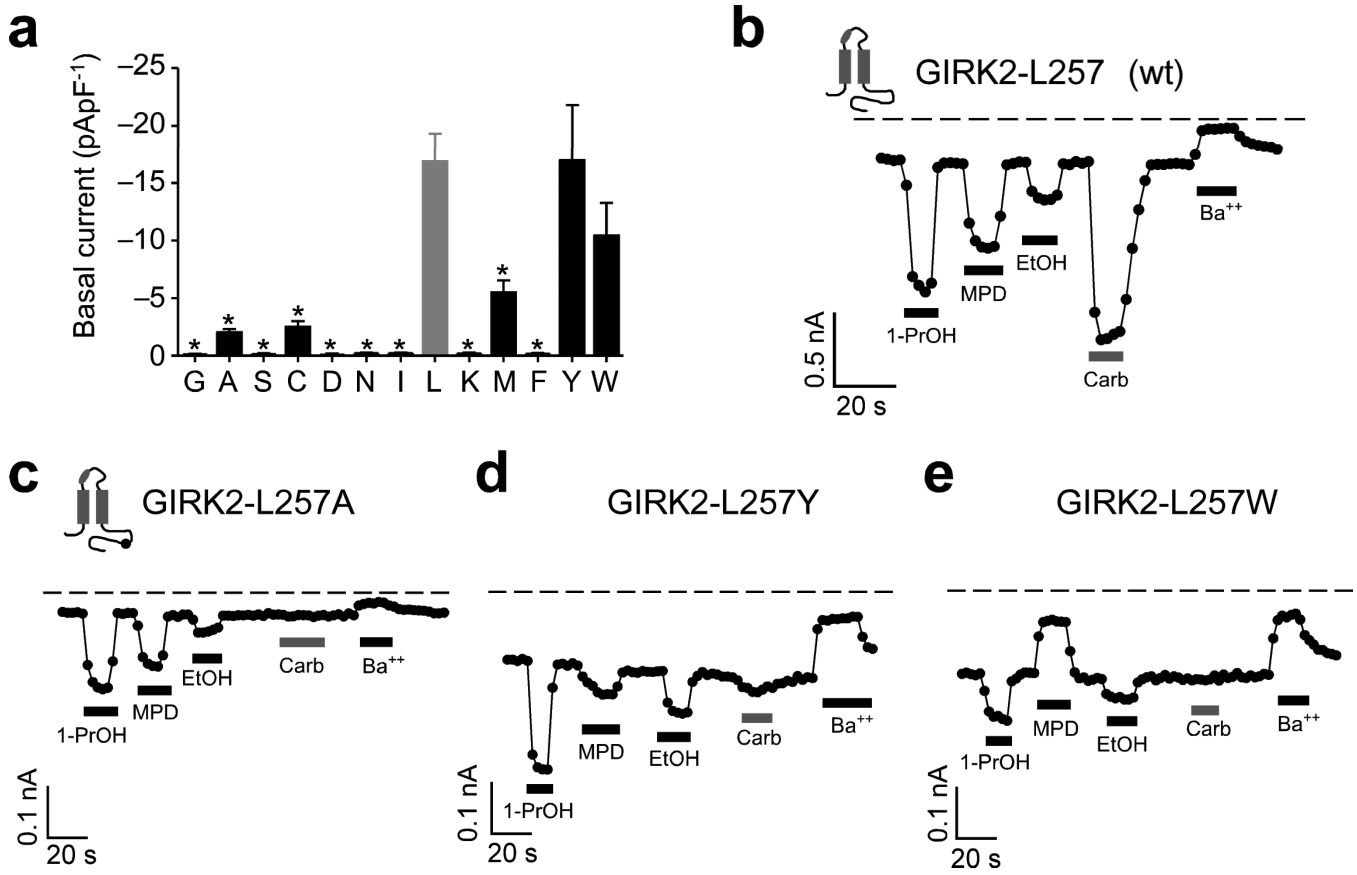

Fig. 4. Comprehensive mutagenesis of GIRK2-L257 in βD-βE ribbon of hydrophobic alcohol-binding pocket reveals changes in alcohol- and Gβγ-activated currents

a) Bar graph shows the mean (± s.e.m.) amplitude of basal K^+ current (Ba^{++}-sensitive) for substitutions of increasing molecular side-chain volume at GIRK2-L257: Gly (n=7), Ala (n=9), Ser (n=7), Cys (n=8), Asp (n=7), Asn (n=6), Ile (n=7), Leu (wt; n=34; grey bar), Lys (n=7), Met (n=8), Phe (n=7), Tyr (n=9) and Trp (n=9). **b-e**) Inward K^+ currents for wild-type GIRK2 (**b**) and the indicated GIRK2-L257 mutants (**c-e**) in response to 100 mM 1-PrOH, 100 mM MPD, 100 mM EtOH, 5 μM carbachol, or 1 mM Ba^{++}. Inset shows the approximate position of the C-terminal mutation.

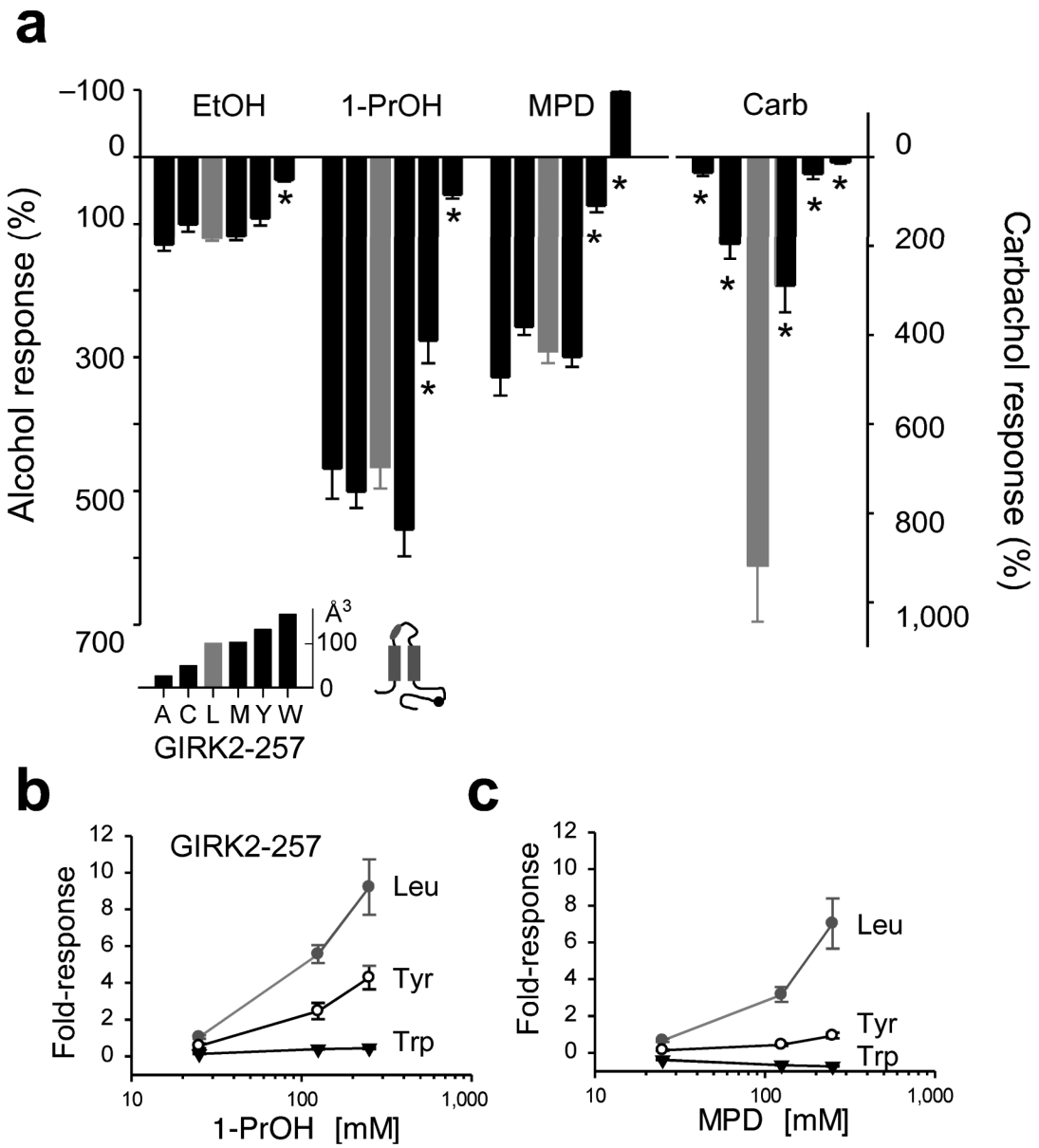

Fig. 5. Reduced alcohol activation with increasing bulkiness of amino acid substitutions at GIRK2-L257

a) Bar graph shows the mean percentage response to different alcohols and carbachol (± s.e.m.), normalized to the basal K^+ current (Ba^{++}-sensitive). Upward response indicates inhibition. Amino acid substitutions are arranged by increasing side-chain volume ($Å^3$, see inset). Asterisk indicates significant statistical difference ($P < 0.05$ vs. Leu). **b,c**) Dose-response curves are shown for GIRK2-L257, GIRK2-L257Y and GIRK2-L257W channels for 1-PrOH (**b**) and MPD (**c**). Note suppression of alcohol activation at all concentrations tested.

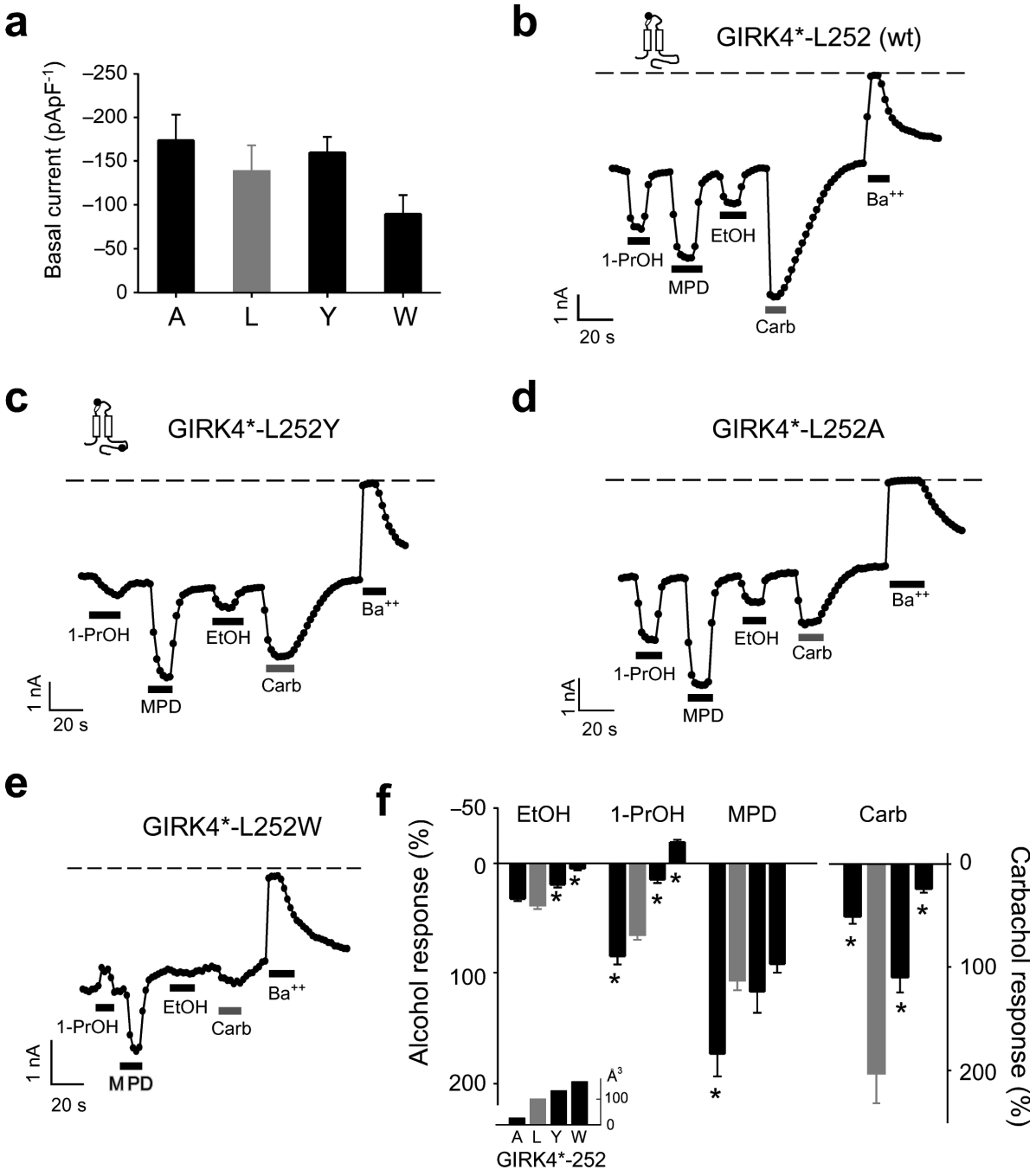

Fig. 6. Mutations in the hydrophobic alcohol-binding pocket of GIRK4* alter alcohol-activated currents

a) Mean basal K^+ currents (Ba^{++}-sensitive) measured for Ala (n=8), Leu (wt; grey bar, n=8), Tyr (n=8), and Trp (n=8) substitutions at GIRK4*-L252. There are no statistical differences in basal currents ($P > 0.05$ vs. Leu). **b-e**) Inward K^+ currents for GIRK4* (**b**) and different GIRK4*-L252 mutants (**c-e**) in response to 100 mM 1-PrOH, 100 mM MPD, 100 mM EtOH, 5 μM carbachol, or 1 mM Ba^{++}. **f**) Bar graphs show the mean percentage responses to different alcohols and carbachol, normalized to the basal K^+ current (Ba^{++}-sensitive).

Amino acid substitutions are arranged by increasing side-chain volume ($Å^3$) (see inset). Asterisk indicates significant statistical difference ($P < 0.05$ vs. Leu). Channel schematics show the approximate position of the pore-helix (white ellipse) mutation, for making GIRK4*, and the C-terminal mutation (black circle). All values are mean ± s.e.m.

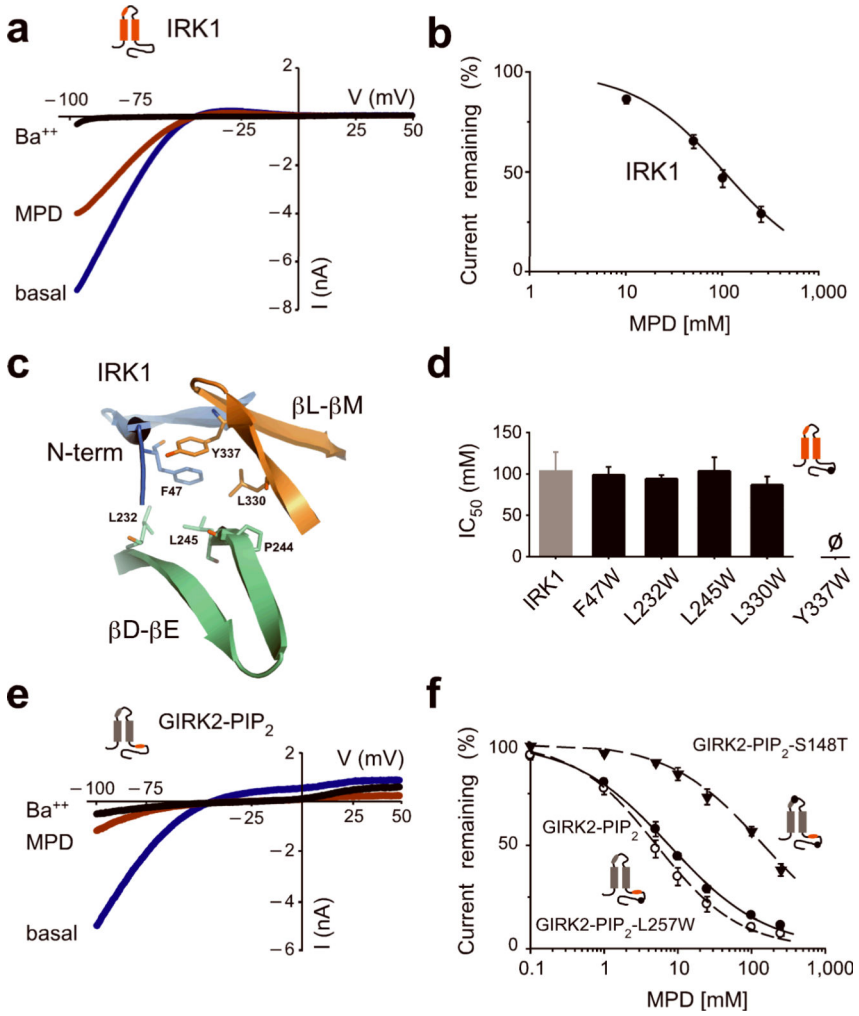

Fig. 7. Mutations in the hydrophobic alcohol-binding pocket of IRK1 have no effect on alcohol-dependent inhibition

a) Current-voltage plots for IRK1 channels are shown for 20K (blue), 20K plus 1 mM Ba^{++} (black) or 20K plus 100 mM MPD (red). MPD inhibited the basal K^+ current (Ba^{++}-sensitive) by 53.1%± 4.1% (n=8). **b**) Dose-response curve is shown for MPD inhibition of IRK1 channel. Smooth curve shows best fit using the Hill equation, with an IC_{50} of 104 ± 23 mM and Hill coefficient of 0.93 ± 0.03 (n=8). **c**) Structural view of amino acids that line the hydrophobic alcohol pocket in IRK1. **d**) Bar graph shows mean IC_{50}'s for MPD-dependent inhibition of IRK1 (n=8), IRK1-F47W (n=7), IRK1-L232W (n=7), IRK1-L245W (n=6), IRK1-L330W (n=6). There is no statistical difference compared to wild-type IRK1 ($P > 0.05$). **e)** Current-voltage plots are shown for GIRK2-PIP_2 (GIRK2 engineered with high affinity PIP_2 binding domain from IRK1) channels recorded in the presence of 20K (blue), 20K plus 1 mM Ba^{++} (black) or 20K plus 100 mM MPD (red). **f**) Dose-response curves for MPD-dependent inhibition of GIRK2-PIP_2 (solid circle), GIRK2-PIP_2-L257W (open circle) and GIRK2-PIP_2-S148T (solid triangle). Smooth curves show best fit using the Hill equation and having IC_{50}'s and Hill coefficients of 7.7 ± 1.0 mM and 0.66 ± 0.03 (n=5) for GIRK2-PIP_2, 5.2 ± 1.0 mM and 0.77 ± 0.04 (n=5) for GIRK2-PIP_2-L257W, and 147.0 ± 31.5 mM and 0.67 ± 0.05 (n=6) for GIRK2-PIP_2–S148T. All values are mean ± s.e.m.

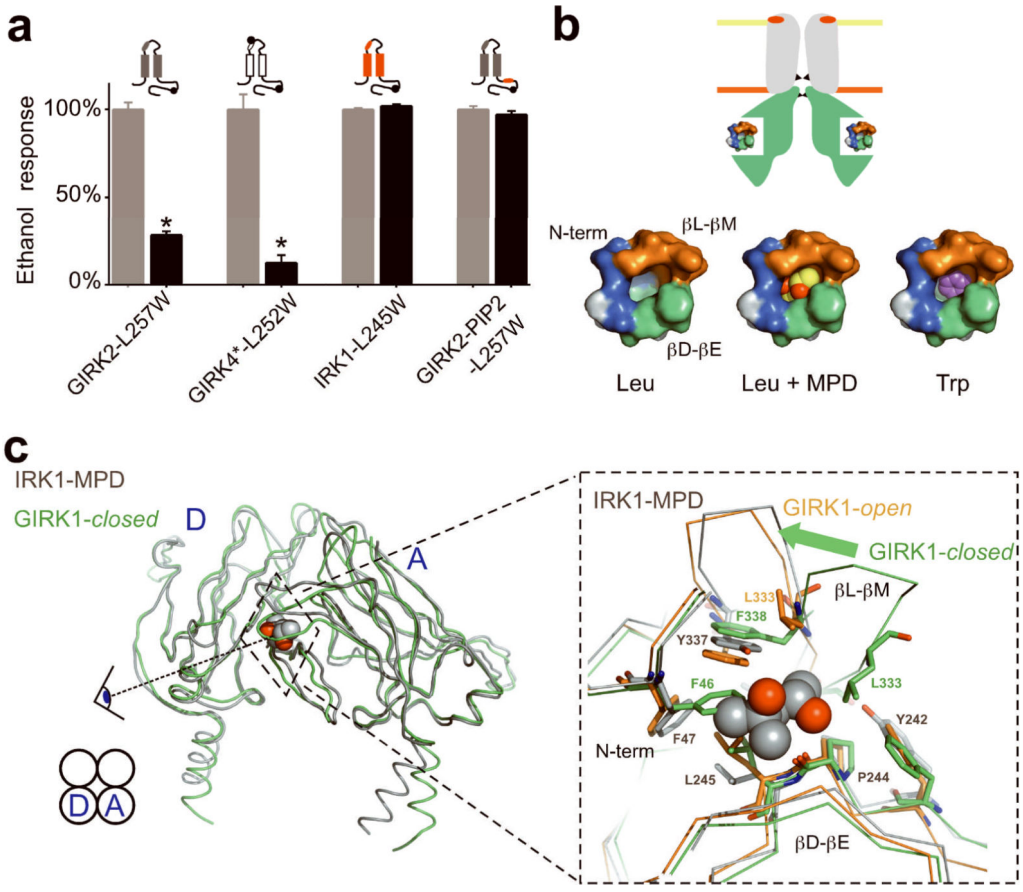

Fig. 8. Model for alcohol-dependent activation of GIRK channels

a) Bar graph shows the mean percentage EtOH response (activation or inhibition normalized to wild-type) for a Trp mutation in four different channels, GIRK2-L257W (n=9), GIRK4-L252W (n=8), IRK1-L245W (n=8) and GIRK2-PIP_2-L257W (n=5). Only mutations in alcohol-binding pocket of wild-type GIRK channels affect the response to alcohol. **b**) Top, schematic of inward rectifier shows location of alcohol-binding pocket in cytoplasmic domains, two gates (G-loop and M2 transmembrane; black triangles) and pore-helix region (red ellipse). PIP_2 is enriched in lower leaflet of bilayer (orange). Below, molecular surface representations of the alcohol pocket without (Leu), with MPD (Leu+MPD) and modeled with L257W (Trp), using the IRK1-MPD structure as a guide. **c)** Left, alignment of the putative closed state of GIRK1 chimeric channel (GIRK1-*closed*; green) (PDB:2QKS) with the IRK1-MPD structure (grey) (PDB:2GIX). Spaghetti structures show two adjacent cytoplasmic subunits (subunits D and A) and the hydrophobic alcohol pocket at the cytoplasmic subunit interface. Right, zoom shows alignment of the N-terminal domain, βD-βE and βL-βM ribbons from the IRK1-MPD (grey), GIRK1-*open* (orange) and GIRK1-*closed* (green) structures. IRK1-MPD aligns better with the putative open state of GIRK1. Note the significant displacement in the βL-βM beta ribbon element (arrow) and the side-chains of hydrophobic amino acids in the two structures. GIRK1-*closed* but not GIRK1-*open* has a collapsed alcohol-binding pocket, due to interaction and rotation of F46 (IRK1-

F47), L246 (IRK1-L245) and F338 (IRK1-Y337). GIRK1-L333 in the βL-βM domain, implicated previously in Gββ gating of GIRK channels17-19, is shown for reference.